

11.7 Interactions of the winter lake-affected boundary layer with synoptic systems

J. Dreher¹, K. Fitzpatrick², M. R. Hjelmfelt*, W.J. Capehart
South Dakota School of Mines and Technology, Rapid City SD

D.A.R. Kristovich
Illinois State Water Survey and University of Illinois, Champaign, IL

J. Schroeder
White Sands Missile Range, NM

1. Introduction

Many papers have been written about lake-affected boundary layers and lake-effect snow storms. However, little research has been published on interactions of these lake-affected boundary layers with synoptic systems. In this presentation we will describe simulations and observations of two such interactions: 1) seeding of lake-effect boundary layer convective clouds over Lake Michigan by snow falling from higher, cyclone-generated cloud layers, and 2) impacts of the lake-affected boundary layer on a synoptic cold front crossing Lake Michigan.

Simulations of 5 December 1997, show that even very light seeding of shallow lake-effect boundary layer clouds produced deeper clouds, enhanced vertical motions, increased precipitation production, and produced larger snow mass concentrations in agreement with observations taken during the Lake-Induced Convection Experiment (Lake-ICE). Simulations further revealed that the snowfall was dominated by the lake-effect clouds, but the very light seeding produced a measurable enhancement.

Cold front interaction with the relatively warm convective lake-effect boundary layer early on 10 January 1998 resulted in a slowing of the frontal progress over the lake, a deepening of the clouds, and increased precipitation from the cold front. Simulations showed that the impacts were dominated by the heat and moisture fluxes from the lake surface rather than surface roughness differences over the lake.

Corresponding author address: Mark Hjelmfelt, Institute of Atmospheric Sciences, SDSM&T, 501 East Saint Joseph Street, Rapid City, SD 57701-3995. E-mail:

Mark.Hjelmfelt@sdsmt.edu

¹Current address: Joseph Dreher, ENSCO, Inc., Aerospace Sciences and Engineering Division, Melbourne, FL 32940

²Current address: Katy Fitzpatrick, Riverton Weather Forecast Office, Riverton, WY 82501

2. Data

The two cases, 5 December 1997 (seeding) and 10 January 1998 (frontal passage), occurred during the Lake-ICE field project. Research data collected during Lake-ICE (Kristovich *et al.* 2000), as well as standard meteorological observations from the National Weather Service network, including WSR-88D radars, are used in this investigation. For the 5 December case, in-situ aircraft measurements obtained by the University of Wyoming King Air and airborne radar observations from the NCAR Electra Doppler Radar (ELDORA) were also utilized.

3. Mesoscale Model

The Penn State University/National Center for Atmospheric Research Fifth Generation Mesoscale Model (MM5), was used in the study. Three nested grids were used for these studies. A coarse grid domain, centered at 44°N and 86°W with a 13.5 km horizontal grid spacing, covered the entire Great Lakes region. A second domain, nested within this domain with a horizontal grid spacing of 4.5 km, covered Lake Michigan and surrounding states. Finally, an inner domain, with a 1.5 km grid spacing, was centered over central Lake Michigan, Fig. 1.

The model was configured using the NOAA Land Surface Model (NOAH LSM), coupled with the Eta planetary boundary layer scheme. Convective parameterizations were used for the outer grid and explicit microphysics parameterizations for the inner grids. Land use and terrain data for the model were obtained from the United States Geological Survey (USGS). Lake-surface temperatures were obtained from the satellite analyses created by the NOAA Great Lakes Environmental Research Laboratory (GLERL).

The coarse domain was initialized using Eta model data analyses (EDAS) enhanced by vertical sounding and surface station data obtained from NCAR data archives. Eta model analyses at three-hour intervals were also used to establish lateral boundary conditions for the outer domain during the entire run. For model runs without Lake Michigan, the water surface properties of Lake Michigan were replaced by land surface values interpolated from surrounding land grid points.

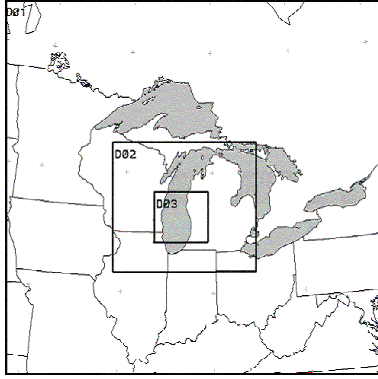


Figure 1: MM5 domains for the model simulations. The outer box (D01) represents the coarse grid centered over the Great Lakes (13.5 km grid spacing). The second box (D02) represents the middle domain, which is centered over Lake Michigan (4.5km grid spacing). The inner box (D03) represents the high-resolution inner

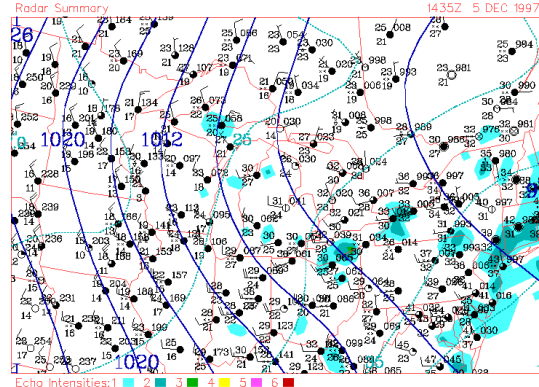


Figure 2: Surface analysis taken at 1500 UTC on 5 December 1997 demonstrating the presence of a shortwave over the northern portion of Lake Michigan (from NCDC – archived by NCAR on JOSS website). Heavy lines correspond to barometric pressure at intervals of 4 hPa; dashed lines indicate temperature (intervals of 5°C). Also shown are locations of precipitation echoes and surface station plots.

4. Natural Seeding of a Lake-Effect Boundary Layer

Clouds associated with a retreating surface low-pressure system located north of Maine (Fig. 2) on 5 December 1997 produced widespread light snow in the Great Lakes region. Bands of precipitation (oriented east to west) associated with the synoptic system periodically moved across Lake Michigan in a southerly direction. As the bands traversed the lake, they interacted with the boundary-layer clouds produced through lake-effect processes. These weak bands were detectable by the WSR-88D radar at Green Bay, WI. Figure 3 shows the location of the upper precipitation echoes along with the location of a stack of level flight legs conducted by the King Air near the time of the radar observations.

Observations

Data collected during Lake-ICE confirmed that precipitation from the upperlevel cyclone-produced clouds was falling into the lower lake-effect clouds. Flight notes indicated visual confirmation of this seeding, and observations from the NCAR Eldora Doppler Radar (ELDORA) showed clear indications, as shown in Fig. 4. This image, which was taken at 1713 UTC, shows a weak area of upper-level precipitation falling into the lower, higher-reflectivity cloud deck. In addition, as the King Air flew above the lake-effect clouds over western portions of Lake Michigan, snow was observed ~50% of the time, while clouds were observed < 5% of the time. These and similar observations at other locations over the upwind half of the lake are indicative of natural seeding.

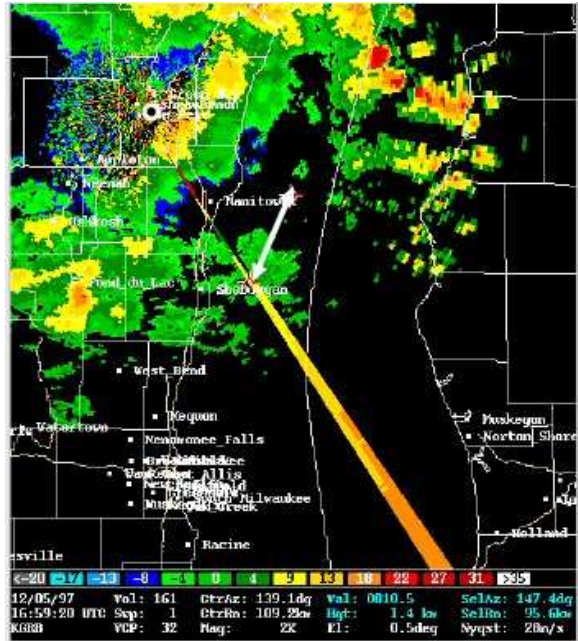


Figure 3: KGRB reflectivity image from 1659 UTC 5 Dec 1997. The King Air's approximate flight path for pass AB3 is indicated by the double arrow. The location of KGRB is indicated by the dark circle at the upper left. A non-precipitation artifact is seen radiating to the southeast of KGRB.

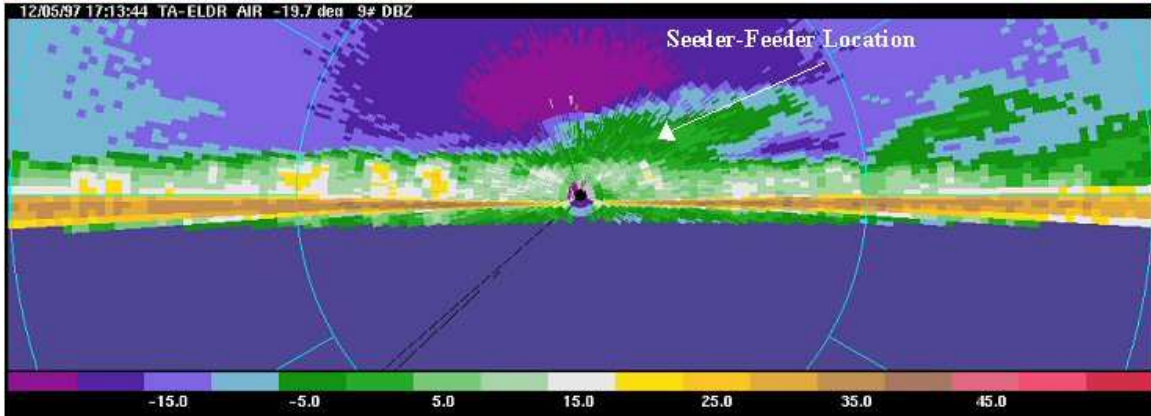


Figure 4: ELDORA image taken at 1713 UTC on 5 December 1997. cross section view with range rings at 10 km. and reflectivity (in dBZ) shaded as given by the color bar. The bottom half (area of blue) represents the surface of Lake Michigan. Seeding from cloud deck aloft is denoted by an arrow and label.

To determine the influences of the seeding process, observations from the King Air in both seeded and non-seeded areas were compared. The WSR-88D-observed reflectivity fields were used to determine areas where precipitation was falling into the lake-effect convection. Aircraft data from these regions were then compared with non-seeded regions to examine differences in boundary layer growth. Schroeder *et al.* (2002) report that results indicated that the local boundary layer in the seeded area was deepened by approximately 15%. Snow size spectra were also examined by Schroeder *et al.* (2002). An example has been reproduced in Fig. 5. The seeded portions of the lower-level cloud were characterized by broader snow spectra than those areas which were not seeded. Concentrations of large particles were increased in the seeded areas. These indicate increased snow mass concentrations and snowfall intensity in the seeded areas.

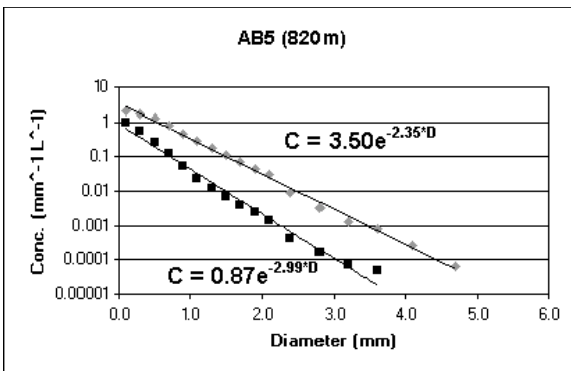


Figure 5: Snow spectra for seeded (gray diamonds) and non-seeded (black boxes) areas as measured by a 2D probe on the King Air on flight path AB in Fig. 3. The best fit lines follow an exponential relationship (from Schroeder *et al.* 2002).

Simulations:

MM5 simulations of this case include a base simulation of the 5 December case and a “No-Lake” run with Lake Michigan removed. The latter simulation generates precipitation that is a direct result of the upper-level low pressure system (lake-effect processes are inactive). Comparisons between this simulation and the base simulation will demonstrate the extent to which the lake-effect processes enhanced the synoptic-scale precipitation. A final simulation entailed modification to the microphysical scheme in the MM5 to remove the falling precipitation from the upper cloud bands at the 700-hPa level, to prevent seeding of the lower, lake-effect clouds.

The base simulation of the 5 December 1997 case successfully showed both seeding and lake-effect precipitation. A vertical cross section of one area of seeding activity can be seen in Fig. 6 for a simulated time of 1730 UTC. This cross section was produced from within the inner domain. The vertical cross section of snow mixing ratio, q_{sn} , has two sets of contours (Fig. 6a). The first of these is the dashed contour which indicates the snow mixing ratio of $0.1 \times 10^{-6} \text{ g kg}^{-1}$. The second set of contours (solid lines) start at $1.0 \times 10^{-3} \text{ g kg}^{-1}$ with an interval of 0.03 g kg^{-1} . The dashed lines nearly touch near $x=28 \text{ km}$, indicative of possible seeding. It was found that in regions indicating seeding, the q_{sn} was deeper (enhanced precipitation processes) and there were higher snow concentrations. The cloud water mixing ratio field, Fig. 6b, illustrates the deepening of the lake-effect cloud decks in the seeded area.

To determine which of the simulations (base, no-lake, or removal of seeding precipitation) produced the greatest snow intensity, a comparison was made of the areas of snow mixing ratio values greater than 2 g kg^{-1} in a seeded region. These

comparisons were made at 1700, 1715, 1730, and 1745 UTC. The area, shown in Fig. 7, covered 4232.25 km² over the lake at 850 hPa. Table 1 shows the aerial coverage for each simulation at each time and the average for each simulation. Results indicate that removal of the lake-effect process (synoptic precipitation only) dramatically decreased the snow concentrations over the lake as no values over 2 g kg⁻¹ were observed. Removal of the seeding from the upper cloud deck also greatly decreased the snow concentrations relative to the base simulation.

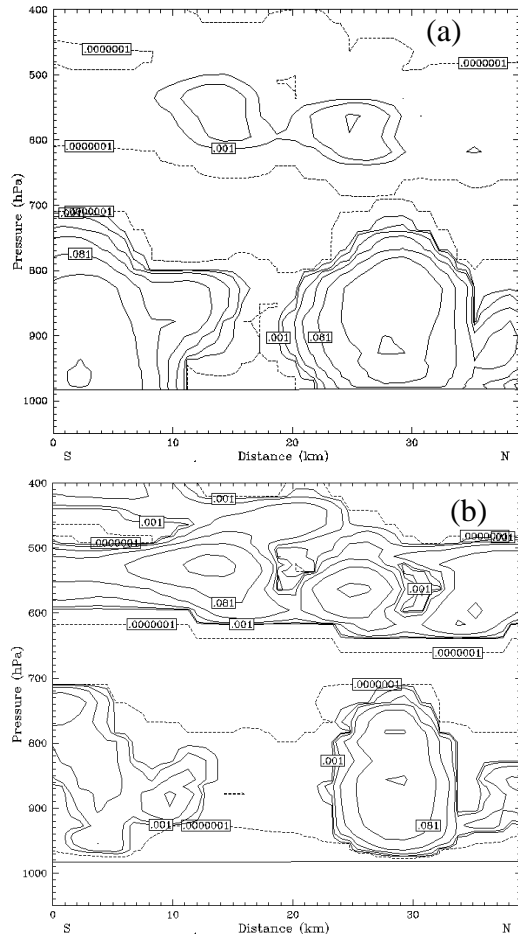


Figure 6: Vertical cross sections at 1730 UTC. Seeding is present at 28km. (a) Snow mixing ratios, (b) Cloud water mixing ratios. The dashed contour indicates the 0.1×10^{-6} with solid contours starting at 0.001 with a contour interval of 0.03 g kg^{-1}

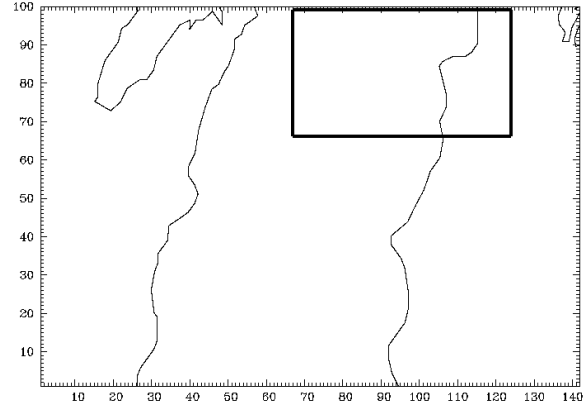


Figure 7: Area where snow mixing ratios greater than 2 g kg^{-1} were calculated (results in Table 1). Area chosen based on its correlation with lake-effect and seeding processes. Axes in units of grid spacings (1.5 km).

Table 1 Comparison of 850 hPa areas of snow mixing ratios greater than 2 g kg^{-1} . Values in units of km².

| UTC | Base (i.e., both lake-effect and synoptic precipitation) | Removal of upper-level Precipitation (i.e., Lake-Effect Only) | Removal of Lake Michigan (i.e., Synoptic Precipitation only) |
|---------|--|---|--|
| 1700 | 12.94 | 0 | 0 |
| 1715 | 24.19 | 9.56 | 0 |
| 1730 | 8.44 | 3.94 | 0 |
| 1745 | 0 | 0 | 0 |
| Average | 11.39 | 3.38 | 0 |

Total precipitation accumulations (between 0000 UTC and 1900 UTC on 5 December 1997) for the base (a) and no-lake (b) and no-seeding (c) simulations are shown in Fig. 8. The contours are in units of mm of water content. Darker shading represents a higher accumulation. The heavier precipitation over the lake area in the base simulation (a) is indicative of the precipitation from the combination of the synoptic and lake-effect precipitation, while the removal of Lake Michigan (b) demonstrates precipitation associated only with the upper-level low pressure system. The higher values of the precipitation east of the lake are due to topographic enhancement on the eastern shores of Lake Michigan. Figure 8a, which shows the surface precipitation accumulation patterns with lake-effect processes allowed, indicates much heavier accumulation for most of the domain, and markedly in-

creased precipitation over the lake. Comparing the base simulation, Fig. 8a, with the no seeding simulation, Fig. 8c, the base simulation shows a mixture of both an areal and narrow banded precipitation, whereas the modified simulation shows more banding, with reduced precipitation amounts in many locations. This comparison demonstrates that, while the precipitation was primarily due to lake-effect processes, the precipitation was enhanced by the upper-level precipitation.

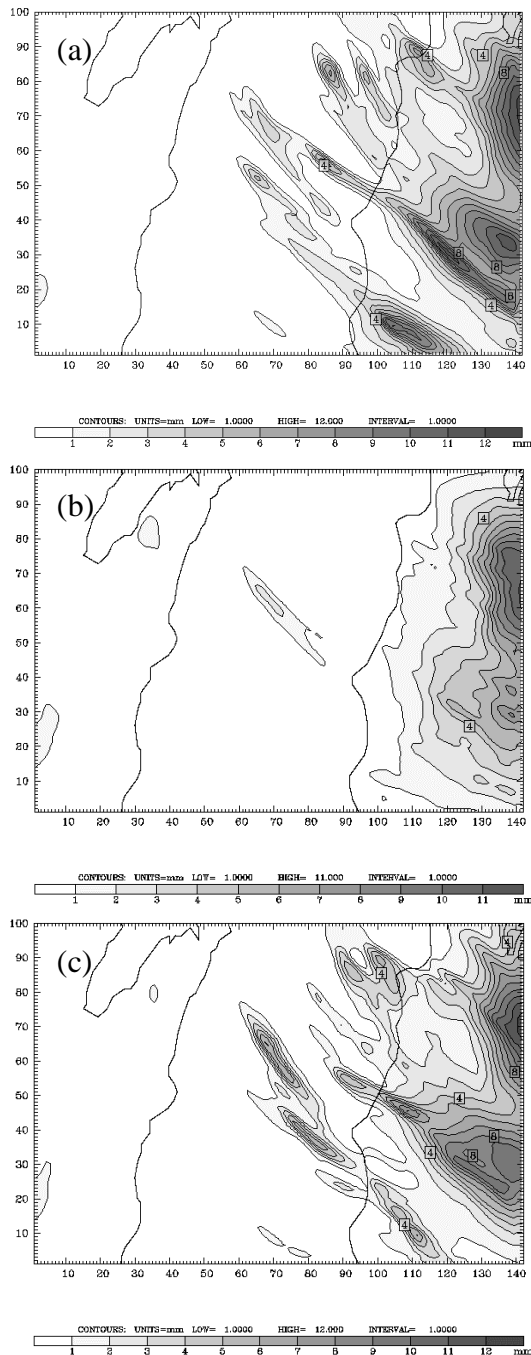


Figure 8: Accumulated precipitation (interval of 1 mm). (a) With Lake Michigan, (b) No Lake Michigan, (c) No seeding precipitation. Darker shading denotes heavier accumulations.

Summary of investigation of effects of natural seeding on a lake-effect boundary layer

Interaction of the lake-effect boundary layer with the precipitating synoptic clouds aloft produced a deeper and more vigorous boundary layer, with greater concentrations of snow, which led to increased snow accumulations.

Further research should be done to investigate the physics of processes involved in the natural seeding scenario to determine the range of physical parameters and meteorological conditions involved. The climatology of these situations is poorly understood, though they must occur frequently as synoptic disturbances recede from the Great Lakes region. Finally the conditions governing the impacts on snowfall need to be studied to provide better guidance for forecasters.

5. The Influence of Lake Michigan on a Winter-time Cold Front

The case of 10 January 1998 provides an example of a relatively shallow arctic front and associated precipitation band crossing the Great Lakes. The arctic front approached the Lake Michigan region and reached the lake around 0300 UTC. The front proceeded across the lake between 0300 UTC and 0600 UTC, bringing strong cold-air advection at the surface, and an associated weak band of precipitation. However, as the front moved across the lake surface, a significant enhancement of the precipitation occurred. As the front moved eastward, away from the lake, the frontal precipitation weakened and classic lake-effect snow developed as arctic air was advected over the warm water.

Observations

Figure 9 depicts approximate locations of the surface cold front as it progressed eastward during 10 January 1998. At 0000 UTC, Fig. 9a, the arctic cold front was located just to the west of Lake Michigan. The boundary was depicted by the west-east temperature gradient, the notable pressure trough extending from the main surface low over southern Ontario, the wind shift line of westerly winds over western Illinois and Wisconsin, and west-southwesterly winds ahead of the boundary. Associated with this frontal zone was a weak area of precipitation located over eastern portions of Wisconsin. At 0535 UTC, Fig. 9b, the arctic boundary had progressed to eastern Lake Michigan. Areas directly east of Lake Michigan remained generally warmer and moister than areas directly west of Lake Michigan as the lake modified the downwind environment. An enhancement of precipitation was evident along the eastern shores of the lake. Note that the front had progressed further eastward south of Lake Michigan, over northern Indiana. Finally, by 1135 UTC, the frontal boundary had pushed into central Michigan (not shown).

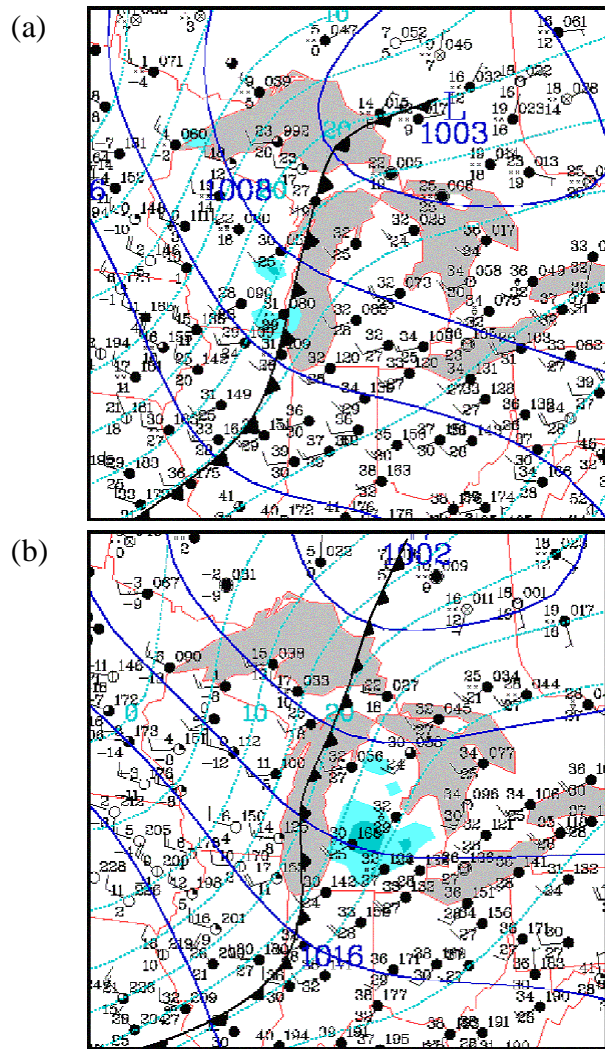


Figure 9. Sea-level pressure composites (interval 2-hPa) and surface temperatures (°F), for 10 January 1998. Dark black line represents approximate location of arctic boundary at (a) 0000 UTC and (b) 0535 UTC. (from NCDC – archived by NCAR on JOSS website).

During this period, Lake Michigan surface temperatures were approximately 2-5°C and ice-free. Ahead of the frontal boundary 850-hPa temperatures were approximately -10°C, indicating a marginally unstable boundary layer. As the surface front crossed the lake, 850-hPa temperatures over the lake did not change significantly. It was not until 1200 UTC that 850-hPa temperatures over the lake dropped to -19°C, which was sufficient to create enough instability for vigorous classic lake-effect snow to develop.

Observations suggest that, as the frontal precipitation band crossed Lake Michigan, an en-

hancement occurred over the central and eastern portions of the lake. For example, Milwaukee, Wisconsin (KMKX), upwind of the lake, reported a trace of snowfall from 2100 UTC 09 January 1998 to 0000 UTC 10 January, as the precipitation band progressed eastward. However, Muskegon, Michigan, downwind of the lake at approximately the same latitude, had 3.8 in of snow from 0000 10 January to 0600 UTC, as the front moved through the region.

Radar cross sections created from the WSR-88D Level II data from Green Bay, WI, and Grand Rapids, MI, illustrate changes in the precipitation band as it crossed the lake. At 2230 UTC 09 January 1998, Fig. 10a, the frontal boundary was slightly to the west of KMKX (approximately 80 km along x-axis). The associated precipitation was relatively weak (peak radar reflectivity of 20 dBz) and shallow in depth. At 0000 UTC 10 January 1998, Fig. 10b, the frontal band had moved across the western portions of Lake Michigan (approximately 120 km along the x-axis). At this time, the precipitation band had increased in intensity, and had grown in depth over the western portions of the lake (130-140 km along x-axis). On the eastern side of the lake, at Grand Rapids, Michigan, KGRR, the greatest enhancement of the precipitation was observed at 0130 UTC, Fig. 10c. Notable in the cross sections were the higher reflectivity returns along the eastern shores of Lake Michigan (approximately 100 km along the x-axis), where the maximum accumulated heat and moisture flux and the greatest frictional convergence is believed to have occurred. At this time a maximum radar reflectivity of 35 dBz was evident just west of KGRR. This area of peak reflectivity was located just ahead of the actual surface frontal boundary.

In summary, observations indicate that significant change in the frontal precipitation had occurred from the time it was located over KMKX to the time it had passed over Lake Michigan. Radar returns were much greater over the lake and in western Lower Michigan than in Wisconsin. The precipitation band also became much deeper as it crossed the lake. Upwind of the lake, maximum radar returns were primarily located below 2 km, Fig. 10a; however, downwind, maximum radar returns extended above 3 km, Fig. 10c. At 0600 UTC, Fig. 10d, the frontal precipitation had weakened as it moved away from the lake surface. An interesting feature evident at this time was a slight eastward tilt, in height, of higher reflectivity returns near KGRR, indicative of a forward tilting cold frontal feature (90 km along x-axis). The forward tilting feature may have represented a slowing of the main frontal boundary closest to the surface, relative to radar returns at 1-2 km, as it moved over the warmer lake surface.

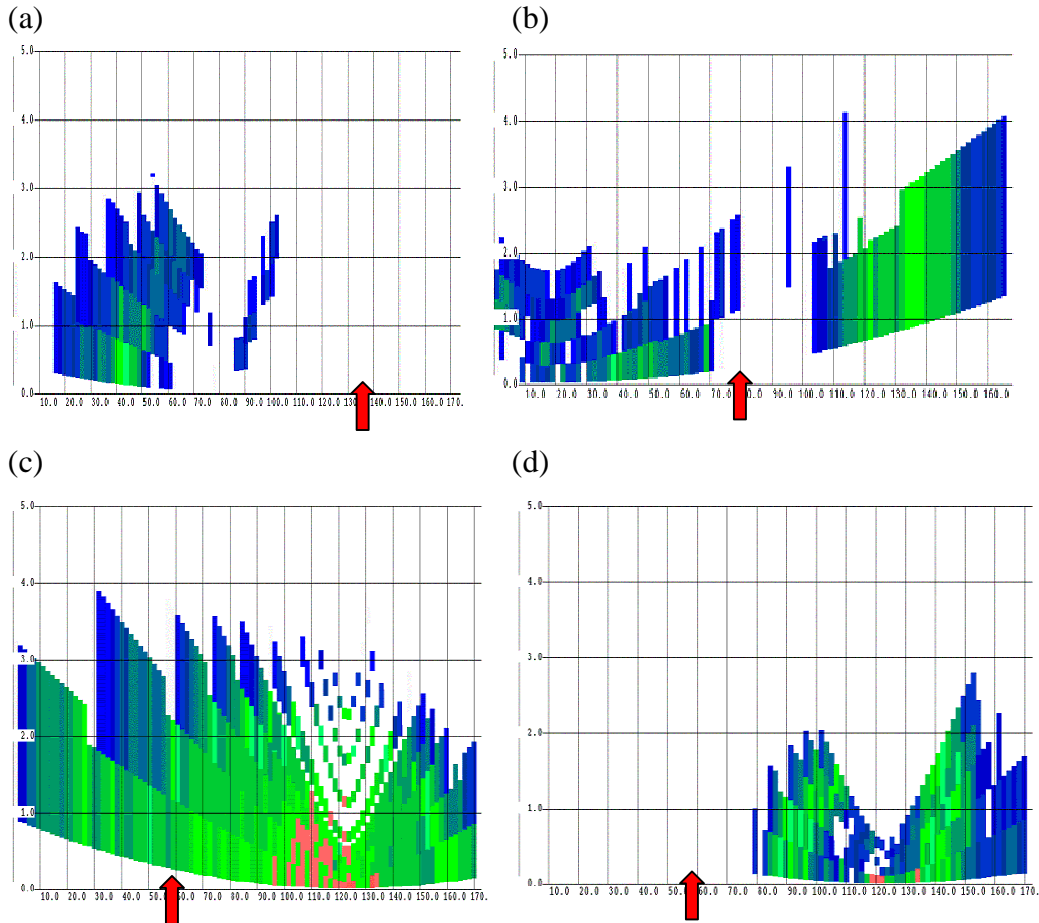


Figure 10: WSR-88D radar cross sections. From KMKX (a) 2230 UTC 9 January, (b) 0000 UTC 10 January 1998. From KGRR (c) 0130 UTC 10 January 1998, (d) 0600 UTC. Red arrow indicates shoreline.

By 1200 UTC, the frontal boundary had progressed east of the region and cold air had deepened enough that lake-effect precipitation was occurring near Lake Michigan (not shown). The convection associated with the lake-effect snow was shallow but intense up to the base of the inversion located at 1-km altitude.

Numerical Simulations

Model simulations include with-lake (WL) and no-lake (NL) simulations to understand the importance of the lake on the simulated atmospheric conditions. A model sensitivity test was also conducted where the surface roughness of Lake Michigan was increased to understand how lake surface roughness impacts frontal speed and structure.

Shown in Fig. 11 are results from the outer domain simulation (13.5 km grid spacing), which indicate sea-level pressure, temperature, and surface wind speeds and direction. At 0000 UTC, the simulated cold front was located just to the west of the lake over eastern Wisconsin for both simula-

tions, Figs. 11a, b. The modification of the frontal boundary was most pronounced by 0600 UTC, Figs. 11c, d. In the WL simulation, the colder air wrapped around the southern portion of the lake forming a bulge in the arctic boundary, Fig. 11c, while over the lake the cold air was slowed. The changes in frontal movement were facilitated by the large temperature gradients between the lake-surface and the overlying colder air. For the NL simulation, Fig. 11d, the entire boundary was more defined and further to the east, located over central Michigan. The wind shift line and pressure trough, in particular, were located further east for the NL simulation.

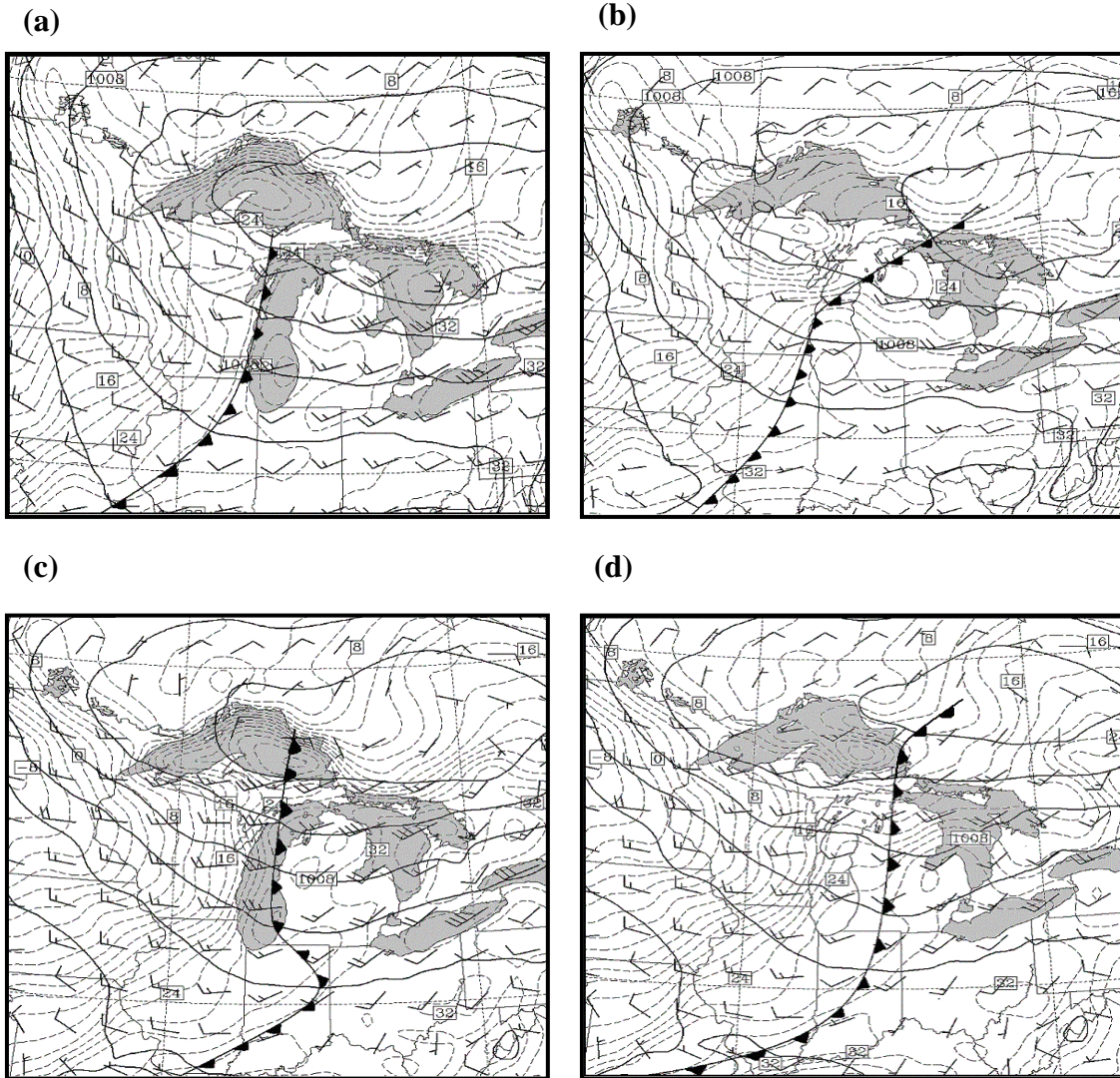


Figure 11. MM5 Outer domain (13.5 km) simulations of sea-level pressure (interval of 4 hPa), 1000-hPa temperature (dashed lines, with interval of 2°F), and 1000-hPa winds (interval of 5 knots). (a) WL simulation (shaded lakes) at 0000 UTC, (b) NL simulation at 0000 UTC, (c) WL simulation at 0600 UTC, (d) NL lake simulation at 0600 UTC.

A higher resolution domain further depicts the modification of the frontal boundary as it migrated across the lake surface. Shown in Fig. 12 are 1000-hPa potential temperatures for the 4.5 km grid. Again, at 0000 UTC, the simulated frontal boundary was just west of Lake Michigan, over central Illinois and Wisconsin (Figs. 12a,b). The actual frontal boundary is depicted by the tight gradient in potential temperature. Ahead of the boundary the surface winds were generally west-southwesterly, while behind the front, the winds were more westerly.

A pronounced slowing of the frontal boundary is evident by 0600 UTC, Fig. 12c, as the thermal ridge was maintained over Lake Michigan and the front had slowly moved east-southeastward. However, for the NL simulation at 0600 UTC, Fig. 12d, the front had progressed into central Michigan and

the arctic air mass (noted by strong gradients over Wisconsin and Illinois) continued to move eastward.

Some enhancement of low-level convergence was evident as the frontal boundary progressed through the region. This occurred over southwestern Michigan as low-level cold air wrapped around the southern tip of Lake Michigan. This is most pronounced in the southwesterly winds that developed along the southern shore of the lake. These southwesterly winds converged with the faster (decrease in surface roughness) westerly winds advecting across the central portions of the lake.

The frontal locations during the period can also be seen in vertical cross sections of potential temperature taken from the inner domain across the lake surface, Fig. 13. The cross sections were taken from point A to B, in Fig. 11a, or roughly perpendicular to the frontal boundary from KMKX to

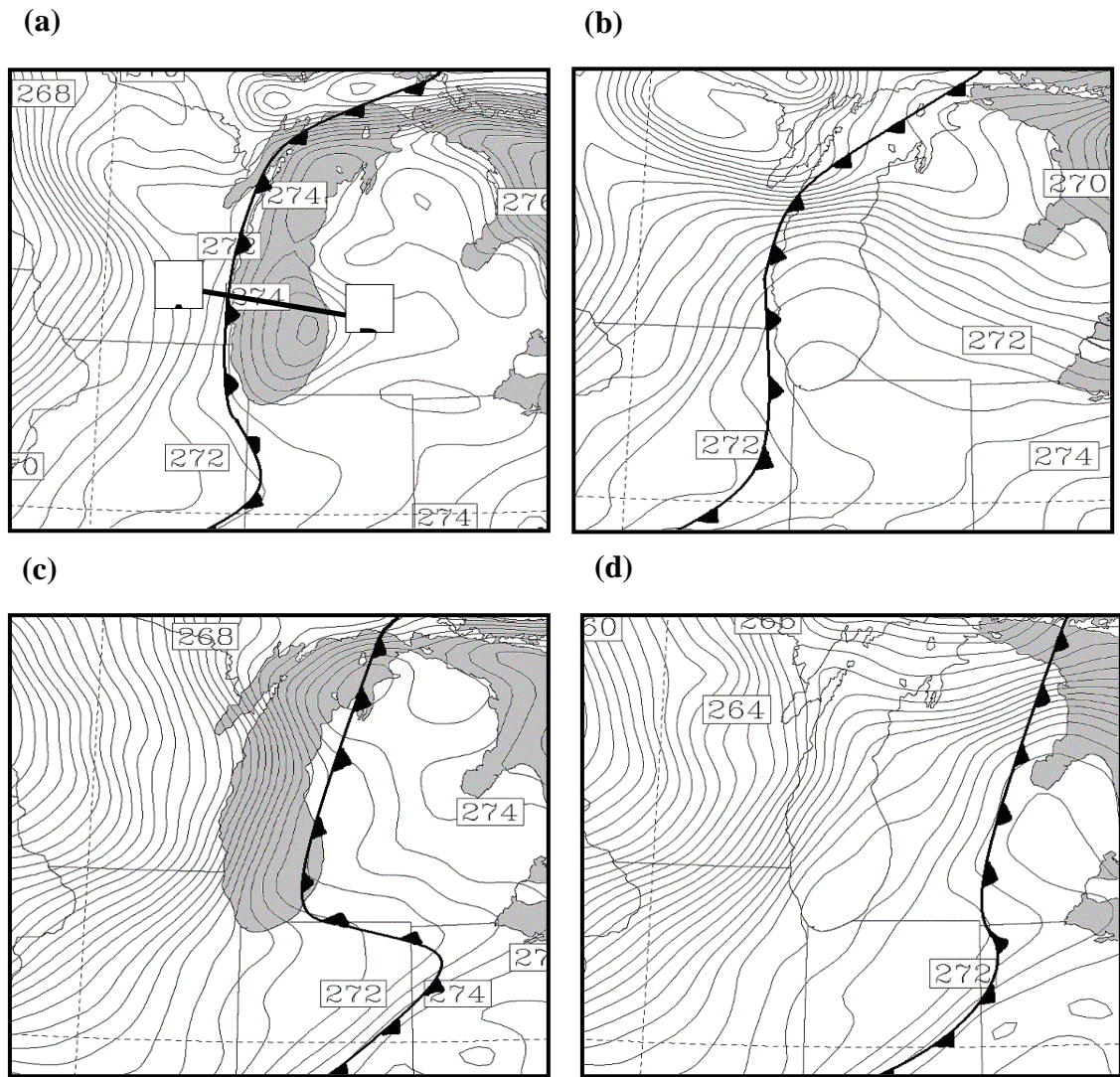


Figure 12: MM5 middle domain (4.5 km) simulations of 1000-hPa potential temperature (interval of 0.5 K). Dark line with barbs represents approximate location of arctic boundary. (a) WL simulation (shaded lakes) at 0000 UTC, (b) NL simulation at 0000 UTC, (c) WL simulation at 0600 UTC, (d) NL simulation at 0600 UTC.

KGRR. The arrows along the x-axis, in Fig. 13, note the approximate location of the arctic boundary.

At 0000 UTC, Fig. 13a, for the WL case, the shallow arctic air behind the frontal boundary was evident west of 130 km below 900 hPa, roughly the height of the inversion base. It appears that the lake surface, from 30-180 km along the x-axis, already had an effect of lifting the capping inversion and mixing away the lowest levels of the cold air, as seen by potential temperature lines increasing with height, in the lowest 20 hPa. For the NL simulation, Fig. 13b, the arctic boundary was located over central portions of the lake, approximately 120-130 km along the x-axis, depicted by the gradual sloping of potential temperature lines from east to west.

By 0600 UTC, for the WL simulation, Fig. 13c, the arctic boundary was near the center of the lake, approximately 130 km along the x-axis, as the cold

air had deepened and progressed eastward from the upper Midwest. Lowering inversion heights associated with the shallow arctic air mass were evident upwind of the lake, and the increasing inversion heights, due to turbulent mixing, were still apparent over the lake itself. Fig. 13d, for the NL simulation, clearly showed the progression of the arctic boundary across the eastern shores of the lake, and no slowing of the frontal boundary (at approximately 160 km along the x-axis). The boundary layer appeared unchanged across the cross section, as enhanced fluxes and turbulent mixing from the lake had not occurred.

Evident in both simulations was a strong temperature inversion located near 800 hPa. This feature was associated with a frontal capping inversion from a cold front that progressed through the Great Lakes 24-h previous to the period of interest, and

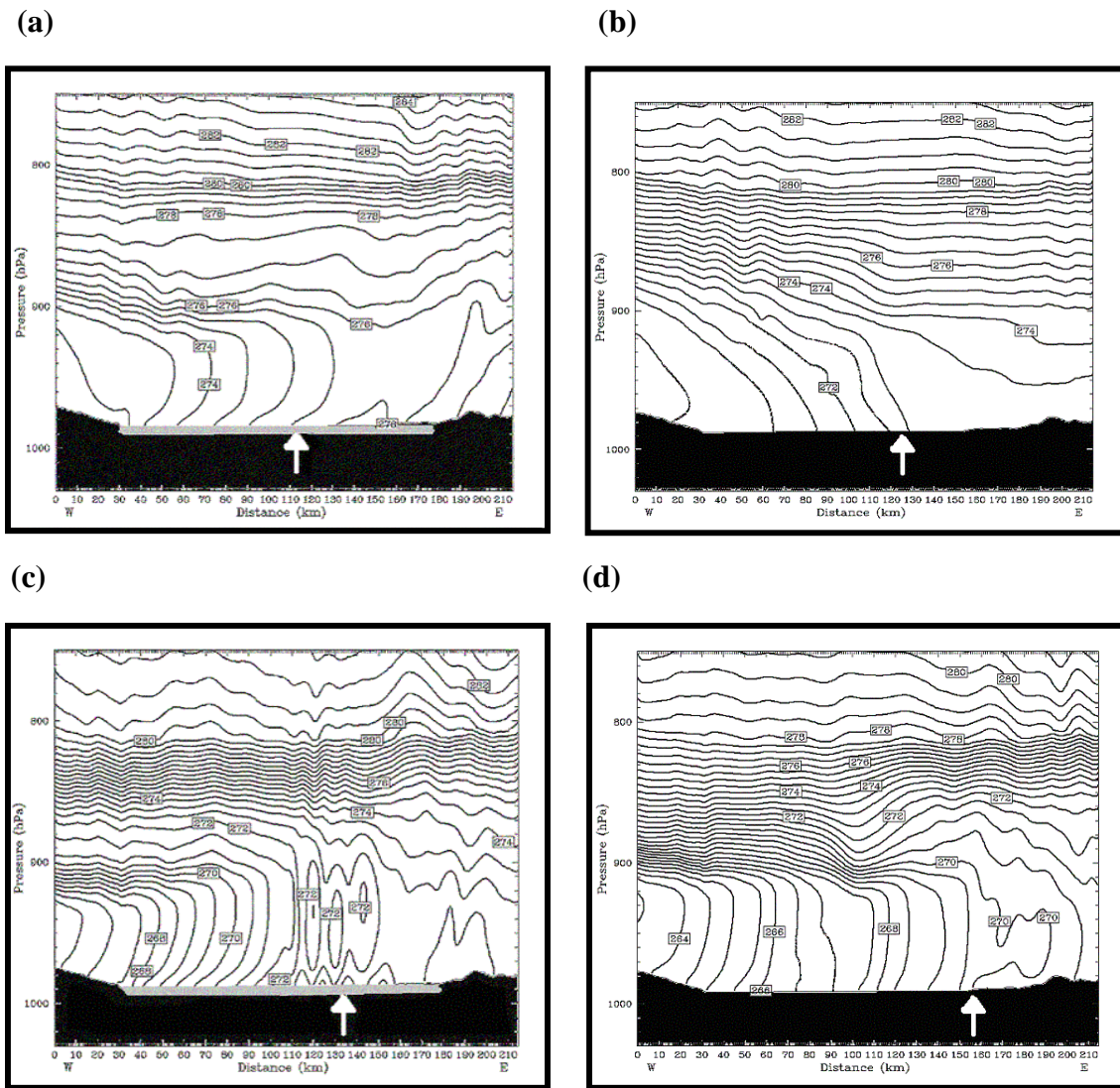


Figure 13: MM5 inner domain (1.5 km) vertical cross sections of potential temperature (K.) Arrow denotes approximate frontal location. (a) WL simulation at 0000 UTC, (b) NL simulation at 0000 UTC, (c) WL simulation at 0600 UTC, (d) NL simulation at 0600 UTC.

hence is not directly related to the low-level features of interest in this study. Also, throughout the period there were enhanced vertical velocities for the WL simulation over the eastern lake and Michigan shores. No enhanced vertical velocities were noted in the NL simulation. By 1100 UTC, the cold air deepened further, the 850-hPa trough crossed the region, the inversion rose, and pure lake-effect snow bands developed.

Finally, as was seen in the radar observations, enhancement of the frontal precipitation occurred as it crossed Lake Michigan. Surface concentrations of snow were consistently greater for the WL simulation, and often approached double the values for the NL simulation over the central and eastern parts of the lake.

Discussion

Based on observations and numerical simulations, Lake Michigan had a substantial impact on

the speed, intensity, and precipitation associated with a cold front.

Synoptic-scale observations suggested a slight deceleration of the frontal boundary over the lake and a strong modification of the arctic air as it progressed over the warm lake. Radar observations from sites both upwind and downwind of Lake Michigan depicted an enhancement of the frontal precipitation band as it crossed the lake. The vertical cross sections also identified structural changes to the precipitation band as it progressed over the lake. MM5 simulations indicated that the precipitation band was modified due to the turbulent heat flux, and added moisture from the lake surface. Enhancement of the precipitation was also influenced by a local convergence maximum that existed over western portions of Michigan, as the arctic air wrapped around the southern tip of Lake Michigan. The frontal band weakened considerably as the front moved further east, away from Lake Michigan. Therefore, due to the presence of the lake, the frontal precipitation band was modified

and enhanced temporarily as it moved over the warm lake.

Gallus and Segal (1999) found that there are two primary mechanisms impacting the speed and intensity of a frontal boundary as it progresses over a lake surface. The first is the change in low-level temperature gradient induced by the lake itself. The second is the change in surface roughness between water and land. For cooler lake surfaces the frontal zone accelerates, which they attributed to a reduction in buoyancy-generated turbulence (Gallus and Segal 1999). This effect would be most pronounced in the springtime, as the lake is generally cooler than the overlying air. However, the 10 January case occurred during a time when lake temperatures were significantly warmer than the surrounding land, and much warmer than the overlying air, such that a significant amount of buoyancy-generated turbulence was generated. The lake also represented an area of surface roughness reduction, as the front moved from over the land to over water. Thus, for the 10 January case, these two mechanisms influencing frontal movement and intensity were competing factors.

Another model run was conducted in which the surface roughness lengths over Lake Michigan were modified to be similar to surrounding land points to test the sensitivity of cold frontal movement to roughness and to distinguish between effects due to lake-induced heating from those due to surface roughness.

Comparison of results to the WL simulation (smaller roughness lengths) showed several differences to the frontal boundary as it progressed across Lake Michigan (not shown). The increased surface roughness slowed wind speeds in the boundary layer, and the simulated cold front moved across the lake at a slower rate than in the original WL simulation and in observations.

Summary of investigation of impacts of a lake-affected boundary layer on a front

These results imply that a combination of lake-induced turbulent heat and moisture flux and an increase in surface roughness (mechanical) acted to slow the progress of the frontal boundary. For the 10 January case, the amount of thermally induced turbulence generated by the warm lake was more than enough to offset the decrease in friction over the lake water and slow the progression of the cold front.

Further study is needed to establish the climatology and investigate lake impacts on deeper more well defined cold fronts and on other types of fronts. More detailed observations are needed of the interaction of the frontal region and the lake-affected boundary layer. Greater understanding of the factors governing lake impacts on fronts is needed to provide forecasting guidance.

Acknowledgements: This work was sponsored by grants from the National Science Foundation

(ATM-- 0202160 and 0202305). Special thanks are also given to Ms. Connie Crandall for help with the publication of manuscript, and Mr. Dick Farley for assistance with NCAR data acquisition. Simulations were performed using the MM5 model which was provided and supported by the Mesoscale Prediction Group in the Mesoscale and Microscale Meteorology Division, NCAR. Satellite imagery was obtained with the help of Dr. Neil Laird. Any opinions, findings, and conclusions or recommendations expressed in this publication are those of the authors and do not necessarily reflect the views of the Illinois State Water Survey.

6. References

- Gallus, W. A., Jr. and M. Segal, 1999: Cold front acceleration over Lake Michigan. *Wea. Forecasting*, **14**, 771-781.
- Kristovich, D. A. R., and co-authors, 2000: The lake-induced convection experiment and the snowband dynamics project. *Bull. Amer. Meteor. Soc.*, **81**, 519-542.
- Schroeder, J.J., D.A.R. Kristovich, and M.R. Hjelmfelt, 2002: The effects of a precipitating winter-time synoptic system on a lake-induced convective boundary layer. AMS: *11th Conference on Cloud Physics Preprints*. 4 pp.